Synthesis of Molded Monolithic Porous Polymers Using Supercritical Carbon Dioxide as the Porogenic Solvent**

By *Andrew I. Cooper* and *Andrew B. Holmes**

Macroporous cross-linked polymers are extremely useful in a wide range of applications.[1] Unlike lightly cross-linked polymers, which become porous when swollen by solvents, macroporous (or "macroreticular") polymers have a permanent porous structure, which is formed during their preparation and persists in the dry state. The internal macroporous morphology is characterized by interconnected channels (pores), which permeate the rigid, extensively cross-linked polymer matrix. Macroporous resins are often synthesized in the form of uniform beads by suspension polymerization;[2] however, this can lead to performance limitations in certain applications, notably the chromatographic separation of large molecules. The passage of molecules within the pores of a macroporous resin is typically controlled by diffusion. Diffusion constants for large molecules, such as proteins or synthetic polymers, are several orders of magnitude lower than for small molecules, causing major problems in applications such as chromatography where the separation efficiency is strongly dependent on mass transfer rates.[3] Modern high-performance liquid chromatography (HPLC) methods frequently involve columns packed with macroporous polymer beads.[4] The flow of the mobile phase between the beads through the large interstitial voids in the column is relatively unimpeded, whereas liquid present in the network of resin pores does not flow and remains stagnant. For large molecule analytes, diffusional mass transfer rates between the interstitial voids and the pores may be very slow, thus causing peak broadening and necessitating low flow rates or longer columns. A very promising approach to this problem has been the synthesis of continuous, macroporous monolithic polymers,[5] which have been developed for a variety of applications,[6] including HPLC,[7] high-performance membrane chromatography (HPMC),[8] capillary electrochromatography,[9] molecular imprinting,[10] and high-throughput bioreactors.[11] Typically, a mold is filled with a polymerization mixture containing a cross-linking monomer, functional comonomers, initiator, and a porogenic diluent. This mixture is then polymerized, either thermally or photochemically, to form a continuous porous monolith that conforms to the shape of the mold. Most systems so far have involved the free radical polymerization of methacrylate- or styrene-based cross-linkers (e.g., ethylene glycol dimethacrylate, divinyl benzene). The porogenic diluent may be either solvating or non-solvating in nature, and carefully chosen ternary solvent mixtures can be used to allow fine control of the porous properties of the monolithic polymers.[9] In some cases, materials have been optimized to incorporate a distribution of small, diffusive pores (<100 nm), interconnected with larger, flow-through pores with diameters in the range 700–2000 nm.[12] The large pores allow sufficient permeability through the monolith and also facilitate convection, thus greatly enhancing mass transport.[6] A key advantage of this methodology is that the macroporous polymers can be prepared directly within a variety of different containment vessels, including both wide bore chromatography columns and narrow bore capillaries.

In this paper we describe for the first time the synthesis of highly cross-linked macroporous polymer monoliths using supercritical carbon dioxide ($scCO_2$) as the porogenic solvent. Carbon dioxide is an attractive solvent for polymer chemistry because it is inexpensive, non-toxic, and non-flammable.[13] Unlike conventional liquid solvents, supercritical fluids (SCFs) are highly compressible and the density (and therefore solvent properties) can be tuned over a wide range by varying pressure. Moreover, SCFs revert to the gaseous state upon depressurization, simplifying the separation of solvent from solute and eliminating solvent residues. DeSimone and others have shown that $scCO_2$ is a versatile medium for both homogeneous and heterogeneous polymerization.[14] Carbon dioxide has also been used for the formation of microcellular polymer foams and aerogels by supercritical fluid processing.[15] Recently, we have demonstrated the synthesis of highly cross-linked polymers by heterogeneous polymerization in $scCO_2$.[16] Dry, free-flowing microparticulate powders of various morphologies were formed, and in all cases the polymers were found to be completely non-porous.[17] We show here that the reaction conditions can be modified to allow the generation of continuous macroporous polymer monoliths in $scCO_2$, and that it is possible to achieve fine control over average pore sizes and pore size distributions.

Previously, we showed that highly cross-linked polymer powders could be formed in $scCO_2$ by the polymerization of cross-linking monomers such as divinylbenzene (DVB), ethylene glycol dimethacrylate (EDMA), and trimethylolpropane trimethacrylate (TRM).[17] The monomer concentration was typically 20 vol.-% or lower, and under these conditions the polymers were isolated as free-flowing, non-porous powders, with particles in the size range 0.4–10 μm. In some cases, uniform polymer microspheres were formed by the use of CO_2-soluble diblock copolymer surfactants.[16,17] In the work described here, we used much higher monomer concentrations (40–60 vol.-%) in order to generate continuous porous polymer monoliths that conformed

[*] Prof. A. B. Holmes, Dr. A. I. Cooper[+]
Melville Laboratory for Polymer Synthesis
Department of Chemistry
University of Cambridge
Pembroke Street, Cambridge CB2 3RA (UK)

[+] Present address: Department of Chemistry, University of Liverpool, Crown Street, Liverpool L69 7ZD, UK.

[**] This research was supported by the Engineering and Physical Sciences Research Council and the EPSRC Mass Spectrometry Service (UK), the Ramsay Memorial Trust (AIC), ICI Acrylics, and the European Union (Brite-Euram contract BRRT-CT98-5089 "RUCADI")

  0935-9648/99/1510-1270 $ 17.50+.50/0

ADVANCED MATERIALS

to the shape of the reaction vessel. The polymerization of TRM and EDMA (Scheme 1) was carried out in $scCO_2$ at various monomer concentrations. The surface areas, median

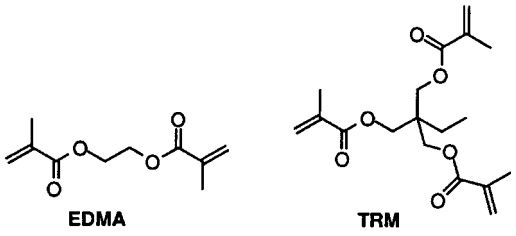

Scheme 1.

pore diameters, total intrusion volumes, and bulk densities for the polymers are listed in Table 1. For polymers formed from TRM, an increase in the monomer concentration led to a marked decrease in the median pore size and a corresponding increase in the specific surface area (samples 1–3). It was found that relatively small changes in the monomer concentration could lead to dramatic changes in the resulting polymer structure. For example, the polymer formed from 40 vol.-% TRM (sample 1) had a median pore diameter of 7880 nm and a specific surface area of 5.2 m^2/g. An increase in the monomer concentration of 10 % led to a product (sample 2) with a median pore diameter of only 100 nm and a specific surface area of 269.4 m^2/g (i.e., 50 times greater than sample 1). Figure 1 shows the pore size distributions for samples 1–3, as measured by mercury intrusion porosimetry. The pore size distributions for samples 1 and 2 were unimodal and narrow (Fig. 1a,b), while the polymer formed using 60 vol.-% TRM (sample 3) had a broader distribution (Fig. 1c), consisting mainly of pores less than 100 nm in diameter. Following IUPAC definitions, samples 1 and 2 would be termed macroporous, while sample 3 is predominantly macroporous but appears to contain a number of pores in the mesopore/micropore size range. The morphology of samples 1–3 was examined by scanning electron microscopy (SEM). Figure 2 shows clearly how the variation in median pore diameter and surface area can be

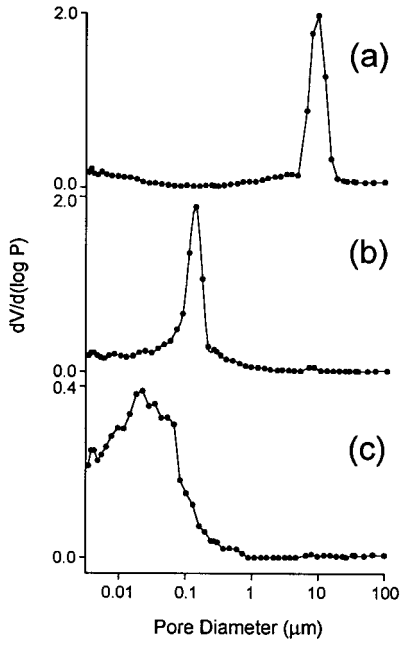

Fig. 1. Effect of monomer concentration on the differential pore size distribution for molded porous monoliths produced in $scCO_2$. Reaction conditions: 50 °C, 12 h, 310 bar, 2 % w/v AIBN. a) Sample 1, 40 vol.-% TRM. b) Sample 2, 50 vol.-% TRM. c) Sample 3, 60 vol.-% TRM.

explained by the internal structure of the polymer monoliths. Sample 1 (Fig. 2a) consisted of relatively large particles, fused together to form an open, porous structure. Samples 2 and 3 (Fig. 2b,c) were found to contain much smaller primary particles which were fused together to form a network of narrower pores. We rationalize this variation in polymer structure by considering the mechanism of formation of the polymeric matrix.[1,18] Carbon dioxide is a very poor solvent for most polymers, with the exception of certain amorphous fluoropolymers and polysiloxanes.[13] In our system, the monomer (TRM) can be considered as a much better thermodynamic solvent for the growing polymer than CO_2. Polymer network phase separation might therefore be expected to occur somewhat later in reactions involving

Table 1. All reactions were carried out in a stainless steel autoclave (10 cm^3 or 40 cm^3) at 50 °C using AIBN (2 % w/v based on monomer).

Sample	Monomer(s)	Vol.-% monomer(s)	Pressure [±10 bar]	Specific surface area [m^2/g] [a]	Median pore diameter [nm] [b]	Total intrusion volume [cm^3/g] [b]	Bulk density [g/cm^3] [b]	Polymer yield [%]
1	TRM	40	310	5.2	7880	0.92	0.49	89
2	TRM	50	310	269.4	100	0.95	0.62	92
3	TRM	60	310	328.3	20	0.53	0.80	98
4	EDMA	40	310	3.2	7860 [c]	1.03	0.43	92
5	EDMA	50	310	5.3	1090 [c]	0.91	0.60	93
6	EDMA	60	310	60.0	130	0.96	0.61	95
7	TRM	50	155	88.8	185	0.95	0.61	95
8 [d]	TRM	50	310	259.6	25	0.68	0.74	98
9 [e]	TRM / MAA	50	310	2.7	2190	0.75	0.64	90

[a] Measured by N_2 adsorption/desorption using the Brunauer–Emmett–Teller method. [b] Measured by mercury intrusion porosimetry over a pore size range 7 nm–100 μm. [c] Bimodal pore size distribution observed. [d] TRM (20 cm^3), H_2O (5 cm^3), AOT (0.2 g), AIBN (0.4 g). [e] TRM (15 cm^3), MAA (5 cm^3), AIBN (0.4 g).

  0935-9648/99/1510-1271 $ 17.50+.50/0

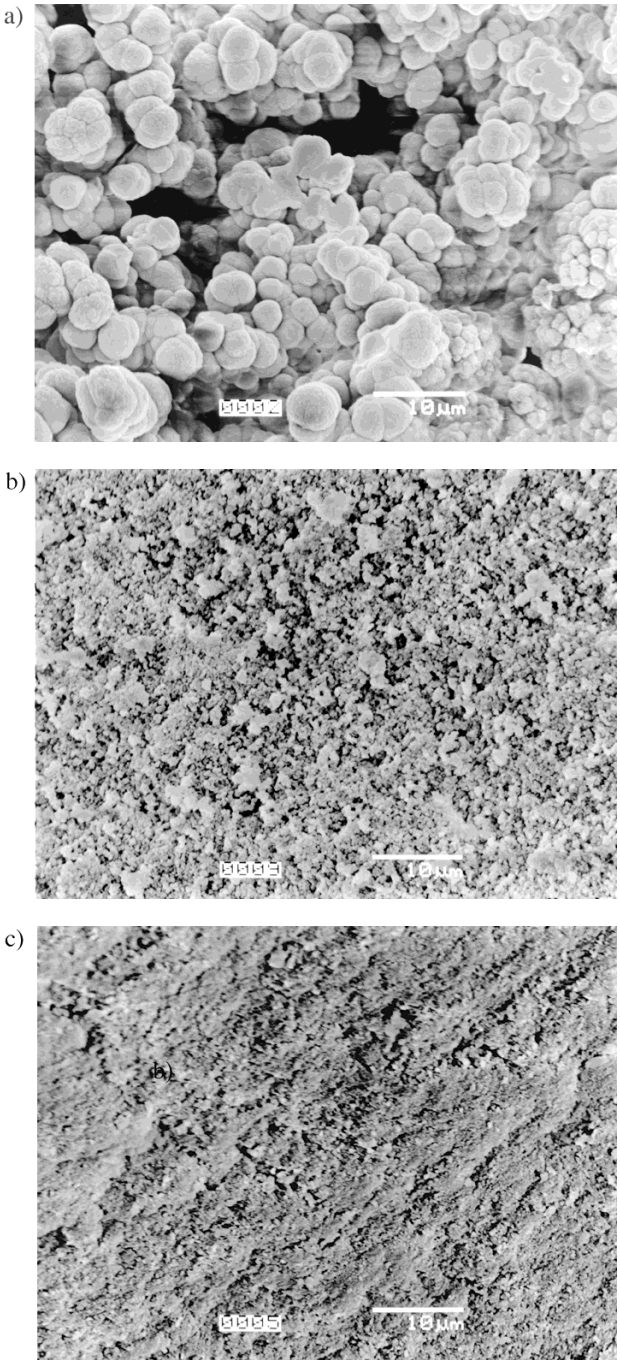

Fig. 2. SEM images showing the internal structure of porous monoliths produced in $scCO_2$ at different monomer concentrations. Reaction conditions: 50 °C, 12 h, 310 bar, 2 % w/v AIBN. a) Sample 1, 40 vol.-% TRM. b) Sample 2, 50 vol.-% TRM; c) Sample 3, 60 vol.-% TRM.

higher monomer concentrations (samples 2 and 3, 50 vol.-% and 60 vol.-% TRM, respectively). Consequently, when phase separation does occur, the microgel particles that are formed remain relatively small and discrete (Fig. 2b,c), and are fused together by further polymerization in the CO_2 phase. At lower monomer concentrations (sample 1, 40 vol.-% TRM), phase separation would be expected to occur at somewhat lower conversions. Again microgel particles are formed, but in this case significantly more polymer is generated after phase separation in both the monomer-swollen microgel particles and in the CO_2 phase. This leads to growth of the particles and in-filling of small pores between particles, thus forming large, fused aggregates with relatively low surface areas (Fig. 2a). If the monomer concentration is reduced even further (≤20 vol.-% TRM), the concentration of polymer becomes too low for the formation of a fused monolith, and the microgel particles appear as a fine powder.[17]

Similar trends were observed for polymers synthesized from EDMA (Table 1, samples 4–6), although average pore diameters were somewhat larger and specific surface areas were correspondingly lower. This is in agreement with our previous studies, where EDMA-based polymer powders synthesized in $scCO_2$ were found to have larger particle sizes and lower surface areas than the TRM-based equivalents.[17] Samples 4 and 5 exhibited bimodal pore size distributions, while sample 6 showed a narrow, unimodal distribution. As might be expected, the mechanical stability of the monoliths improved with increasing monomer concentration: samples 1 and 4 were easily crushed to form chalky powders, while samples 2, 3, 5, and 6 were isolated as hard, brittle monoliths, which fractured into millimeter-sized pieces when broken. The polymers were white and opaque in appearance but were found to become translucent when swollen with a solvent (e.g., toluene). The samples could absorb 80–140 % of their weight in solvent when soaked in toluene for 2 h. Interestingly, swelling with toluene tended to cause the monoliths to expand and break apart, whereas this was not observed when the polymers were re-exposed to $scCO_2$. The latter is important since one of our primary goals is to prepare materials for applications that involve supercritical fluid solvents. Bulk polymer densities ranged between 0.5–0.8 g/cm^3 depending on the sample morphology (Table 1), although it should be remembered that mercury intrusion porosimetry does not account for the volume of pores with diameters of less than about 7 nm. This would tend to affect bulk density and total intrusion volume measurements, mostly for samples 3, 6, and 8 which had a certain percentage of pores with diameters in this size range. Absolute (or "skeletal") density, ρ_{abs}, was measured by helium pycnometry, and this did not appear to vary significantly with polymer morphology (ρ_{abs} = 1.30 ± 0.05 g/cm^3 for TRM polymers; ρ_{abs} = 1.55 ± 0.05 g/cm^3 for EDMA polymers).

It is clear that the ratio of solvent to monomer has a very pronounced effect on the pore size distribution of the polymers. Preliminary results suggest that pressure has a more subtle influence on polymer morphology. The polymer prepared from 50 vol.-% TRM at 155 bar (sample 7) was found to have a narrow, unimodal pore size distribution that peaked at 185 nm, somewhat higher than the median pore diameter of 100 nm for the same polymer synthesized at 310 bar (sample 2). This suggests that it might be possible to "fine tune" the pore size distribution by changing the

  0935-9648/99/1510-1272 $ 17.50+.50/0

ADVANCED MATERIALS

pressure, which in turn changes the solvent strength of the supercritical medium.[13] This is analogous to varying the pore size by changing porogenic solvent composition, and our early results are in accordance with previous studies where a decrease in the porogenic solvent strength led to larger average pore diameters.[18]

Another method for the control of pore size distributions in cross-linked polymers is "reverse micellar imprinting", as described by Zhu et al.[19] We have shown that this can be achieved in $scCO_2$ by polymerizing TRM in the presence of an aqueous microemulsion, which acts as a template for pore formation. When TRM was polymerized at 50 vol.-% in $scCO_2$ (sample 2), the pore size distribution was narrow and unimodal, peaking at 100 nm (Fig. 1b). When this experiment was repeated in the presence of a water-in-CO_2 microemulsion (sample 8) stabilized by sodium bis(2-ethylhexyl) sulfosuccinate (AOT), the pore size distribution was significantly broader and shifted to include a wide range of pores with much smaller diameters (median pore diameter = 25 nm). Before polymer phase separation, a clear, transparent aqueous microemulsion was observed in the reaction vessel. Previous studies have shown that it is very difficult to form stable aqueous microemulsions in pure $scCO_2$ by using conventional surfactants, and highly fluorinated stabilizers have usually been required.[20] The stability of the microemulsions in our experiments was presumably a result of the high concentration of monomer in the CO_2 phase.

In order to generate a functional porous monolith, methacrylic acid (MAA) was chosen as a comonomer in the polymerization of TRM (sample 9). The copolymer was found to have a larger median pore diameter than the analogous TRM homopolymer (sample 2), leading to a lower surface area. The formation of materials such as sample 9 suggests that our methods may have potential for the formation of well-defined, non-covalently imprinted monoliths,[10] particularly since CO_2 is a non-polar, aprotic solvent, which, like perfluorocarbons, should not interfere with most template–comonomer interactions.[21] In addition, there is some evidence that the formation of molecular imprints is favored at elevated pressures.[22]

We conclude that it is possible to synthesize well-defined, highly porous cross-linked monoliths using $scCO_2$ as a non-solvating porogenic diluent. We have demonstrated the synthesis of polymers with narrow, unimodal pore size distributions, without the use of complex ternary solvent mixtures. The separation of solvent from polymer is very simple, and no solvent residues are left in the polymer after depressurization. This may be useful, for example, in the formation of molded macroporous polymers within narrow bore capillaries, where the removal of the porogenic solvent can be difficult. Preliminary results show that it is possible to fine-tune the pore size distribution with pressure or by reverse micellar imprinting. The copolymerization of a functional monomer has been demonstrated, which suggests future applications such as molecular imprinting, chromatographic separations, or polymer-supported catalysis. We believe that our methods may be applied to the synthesis of a wide range of porous materials, and that the approach may be particularly valuable for the preparation of specialized cross-linked porous materials for applications that involve subsequent re-exposure to supercritical fluid solvents.

Experimental

High-pressure reactions were carried out in a stainless steel reactor (either 10 cm^3 or 40 cm^3), equipped with a sapphire window for observation of phase behavior [16,17]. In a typical polymerization, the reactor was charged with monomers, initiator (2,2′-azobisisobutyronitrile (AIBN), 2 % w/v based on monomer), and the system was purged with a slow flow of CO_2 for 15 min. The reactor was then pressurized with liquid CO_2 (22 ± 2 °C, 100 ± 5 bar) and stirring (poly(tetrafluoroethylene), PTFE stir bar) was commenced, whereupon the monomer(s) and initiator were observed to dissolve over a period of a few minutes to form a clear solution. Stirring was ceased once the solution had become fully homogeneous. The reactor was then heated to achieve the required reaction conditions (50 °C, 310 ± 10 bar) and left overnight. After cooling to around 40 °C, the CO_2 was vented slowly while still under supercritical conditions. (Safety note: Due to the nature of the porous monolithic products, it is possible that residual pressure could be trapped within the polymer matrix. To minimize this risk, the system was typically allowed to vent overnight before opening the reactor.) The polymers were removed from the reactor as dry, white, continuous monoliths.

For analysis [23], the monoliths were crushed and sieved to a particle size of greater than 2 mm, in order to eliminate any contribution from fine powder. Pore size distributions were recorded by mercury intrusion porosimetry using a Micromeritics Autopore II 9220 porosimeter. Samples were subjected to a pressure cycle starting at approximately 0.5 psia (73 MPa), increasing to 60 000 psia (8.7×10^6 MPa) in predefined steps to give pore size/pore volume information. Polymer surface areas were measured using the Brunauer–Emmett–Teller (BET) method with a Micromeritics ASAP 2010 nitrogen adsorption analyzer. All samples were outgassed overnight at 60 °C under vacuum before analysis. Absolute densities were determined using a Micromeritics Accupyc 1330 helium pycnometer. Polymer morphologies were investigated with a JEOL JSM-5800 LV SEM. Samples were mounted on aluminum studs using adhesive graphite tape and sputter coated with approximately 10 nm gold before analysis.

Received: April 13, 1999
Final version: July 13, 1999

[1] D. C. Sherrington, *Chem. Commun.* **1998**, 2275.
[2] E. Vivaldo-Lima, P. E. Wood, A. E. Hamielec, A. Penlidis, *Ind. Eng. Chem. Res.* **1997**, *36*, 939.
[3] K. Robards, P. R. Haddad, P. E. Jackson, *Principles and Practice of Modern Chromatographic Methods*, Academic, London **1994**.
[4] K. Lewandowski, F. Svec, J. M. J. Fréchet, *J. Appl. Polym. Sci.* **1998**, *67*, 597.
[5] F. Svec, J. M. J. Fréchet, *Anal. Chem.* **1992**, *64*, 820.
[6] F. Svec, J. M. J. Fréchet, *Science* **1996**, *273*, 205. F. Svec, J. M. J. Fréchet, *Ind. Eng. Chem. Res.* **1999**, *38*, 34.
[7] Q. Ching Wang, F. Svec, J. M. J. Fréchet, *Anal. Chem.* **1993**, *65*, 2243. M. Petro, F. Svec, I. Gitsov, J. M. J. Fréchet, *Anal. Chem.* **1996**, *68*, 315. S. Xie, F. Svec, J. M. J. Fréchet, *J. Chromatogr. A* **1997**, *775*, 65.
[8] M. B. Tennikov, N. V. Gazdina, T. B. Tennikova, F. Svec, *J. Chromatogr. A* **1998**, *798*, 55.
[9] E. C. Peters, M. Petro, F. Svec, J. M. J. Fréchet, *Anal. Chem.* **1997**, *69*, 3646. E. C. Peters, M. Petro, F. Svec, J. M. J. Fréchet, *Anal. Chem.* **1998**, *70*, 2288. E. C. Peters, M. Petro, F. Svec, J. M. J. Fréchet, *Anal. Chem.* **1998**, *70*, 2296.
[10] J. Matsui, T. Kato, T. Takeuchi, M. Suzuki, K. Yokoyama, E. Tamiya, I. Karube, *Anal. Chem.* **1993**, *65*, 2223. J. H. G. Steinke, I. R. Dunkin, D. C. Sherrington, *Macromolecules* **1996**, *29*, 407. L. Schweitz, L. I. Andersson, S. Nilsson, *Anal. Chem.* **1997**, *69*, 1179.
[11] M. Petro, F. Svec, J. M. J. Fréchet, *Biotechnol. Bioeng.* **1996**, *49*, 355.
[12] F. Svec, J. M. J. Fréchet, *Chem. Mater.* **1995**, *7*, 707.

  0935-9648/99/1510-1273 $ 17.50+.50/0

[13] M. A. McHugh, V. J. Krukonis, *Supercritical Fluid Extraction*, 2nd ed., Butterworth-Heinemann, Stoneham, MA **1994**.
[14] J. M. DeSimone, Z. Guan, C. S. Elsbernd, *Science* **1992**, *257*, 945. J. M. DeSimone, E. E. Maury, Y. Z. Menceloglu, J. B. McClain, T. J. Romack, J. R. Combes, *Science* **1994**, *265*, 356. A. I. Cooper, J. M. DeSimone, *Curr. Opin. Solid State Mater. Sci.* **1996**, *1*, 761. J. L. Kendall, D. A. Canelas, J. L. Young, J. M. DeSimone, *Chem. Rev.* **1999**, *99*, 543.
[15] S. K. Goel, E. J. Beckman, *Polym. Eng. Sci.* **1994**, *34*, 1137. S. K. Goel, E. J. Beckman, *Polym. Eng. Sci.* **1994**, *34*, 1148. K. L. Parks, E. J. Beckman, *Polym. Eng. Sci.* **1996**, *36*, 2404. K. L. Parks, E. J. Beckman, *Polym. Eng. Sci.* **1996**, *36*, 2417. Y. P. Fu, D. R. Palo, C. Erkey, R. A. Weiss, *Macromolecules* **1997**, *30*, 7611. K. A. Arora, A. J. Lesser, T. J. McCarthy, *Macromolecules* **1998**, *31*, 4614. D. A. Loy, E. M. Russick, S. A. Yamanaka, B. M. Baugher, K. J. Shea, *Chem. Mater.* **1997**, *9*, 2264.
[16] A. I. Cooper, W. P. Hems, A. B. Holmes, *Macromol. Rapid Commun.* **1998**, *19*, 353.
[17] A. I. Cooper, W. P. Hems, A. B. Holmes, *Macromolecules* **1999**, *32*, 2156.
[18] C. Viklund, F. Svec, J. M. J. Fréchet, K. Irgum, *Chem. Mater.* **1996**, *8*, 744. C. Viklund, E. Pontén, B. Glad, K. Irgum, P. Hörstedt, *Chem. Mater.* **1997**, *9*, 463.
[19] X. X. Zhu, K. Banana, R. Yen, *Macromolecules* **1997**, *30*, 3031. X. X. Zhu, K. Banana, H. Y. Liu, M. Krause, M. Yang, *Macromolecules* **1999**, *32*, 277.
[20] K. P. Johnston, K. L. Harrison, M. J. Clarke, S. M. Howdle, M. P. Heitz, F. V. Bright, C. Carlier, T. W. Randolph, *Science* **1996**, *271*, 624.
[21] A. G. Mayes, K. Mosbach, *Trends Anal. Chem.* **1997**, *16*, 321.
[22] B. Sellergen, C. Dauwe, T. Schneider, *Macromolecules* **1997**, *30*, 2454.
[23] Mercury porosimetry measurements were carried out by K. Muoio at Delta Analytical Instruments, Inc., North Huntingdon, PA, USA. Helium pycnometry was carried out by K. G. Brocklehurst and A. Booth at ICI Technology, Runcorn, UK. Nitrogen adsorption/BET analysis was performed by Z. Saracevic in the Department of Chemical Engineering, University of Cambridge, UK.

Electric Field and Wavelength Dependence of Charge Carrier Photogeneration in Soluble Poly(*p*-phenylenevinylene) Derivatives**

By *Thomas K. Däubler*, *Vera Cimrová*,* *Steffen Pfeiffer*, *Hans-Heinrich Hörhold*, and *Dieter Neher**

The photogeneration of charge carriers in conjugated polymers such as poly(*p*-phenylenevinylene) (PPV) is of potential interest for applications in photoreceptors, photodiodes, and solar cells. Despite intensive research, absolute values and, in particular, the mechanism of charge carrier photogeneration in PPVs are still subjects of controversy.[1–9] A band-to-band transition into free carriers, the direct field-induced dissociation of the singlet exciton, as well as the dissociation of a thermalized charge transfer state have been discussed. Moses et al. performed steady-state photoconductivity experiments on sandwich samples of poly(5-(2′-ethylhexyloxy)-2-methoxy-1,4-phenylenevinylene) (MEH-PPV).[5] They concluded that the observed temperature as well as the field dependence of the photocurrent is due to the transport of the photogenerated charge carriers and that the photogeneration mechanism is consistent with a direct band-to-band transition. A low photogeneration efficiency of only 0.1 % was reported. Work by Friend and co-workers on MEH-PPV sandwich cells revealed a pronounced wavelength dependence of the photocurrent quantum yield.[6] It was concluded that the nature of the initially excited excitonic state determines the efficiency for charge carrier photogeneration. These conclusions have, however, been extracted from stationary photoconductivity measurements on thin polymer films sandwiched between two electrodes. In this geometry, external effects might affect the photocurrent through the sample.[7,8,10] Bässler and co-workers demonstrated that high photocurrent quantum yields might be caused by photoinduced electron transfer processes at the interface between the polymer and the electrodes.[7,8] Results of experiments performed under certain conditions could, however, be attributed to bulk photoionization. The pronounced field dependence of the generation efficiency for several PPV derivatives was explained by Onsager's theory for the dissociation of coulombically bound electron–hole (e–h) pairs. Our recent work on photoconductivity of sandwich cells of poly (phenylimino-1,4-phenylene-vinylene-2,5-dioctyloxy-1,4-phenylenevinylene 1,4-phenylene) (PA-PPV) indicated that different photoconductivity gain mechanisms contribute to the photocurrent depending on the thickness of the polymer layer and on the experimental conditions.[10,11] Taking these mechanisms into account, photogeneration efficiencies of approximately 0.6 % at a field of 6.5 V/μm were found.

Here, we report on the determination of the charge carrier photogeneration efficiency η in PA-PPV (**1**) and MEH-PPV by means of emission-limited photoinduced xerographic discharge (XD).[12] Under emission-limited conditions, the photoinduced discharge quantum efficiency η' is independent of both sample thickness and light intensity and equals η. Using this technique, the photoinjection and other problems connected with a second electrode can be

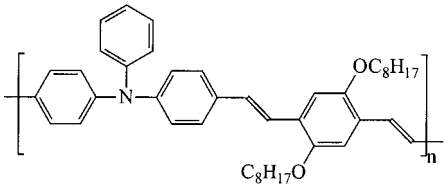

1

[*] Dr. V. Cimrová
Institute of Macromolecular Chemistry
Academy of Sciences of the Czech Republic
CR-16206 Prague 6 (Czech Republic)
T. K. Däubler, Prof. D. Neher
Max-Planck-Institut für Polymerforschung
Ackermannweg 10, D-55128 Mainz (Germany)
Dr. S. Pfeiffer, Prof. H.-H. Hörhold
Institut für Organische Chemie und Makromolekulare Chemie
Universität Jena
Humboldtstrasse 10, D-07743 Jena (Germany)
Prof. D. Neher
Insitut für Physik/Experimentalphysik, Universität Potsdam
Am Neuen Palais 10, D-14469 Potsdam (Germany)

[**] We thank Prof. H. Bässler for helpful discussions. We also acknowledge support by Prof. G. Wegner, MPIP Mainz, by the Volkswagen Foundation and by the Grant Agency of the Czech Republic (Grant No. 102/98/0696).

  0935-9648/99/1510-1274 $ 17.50+.50/0